Liquid Crystals
Publication details, including instructions for authors and subscription information:
http://www.informaworld.com/smpp/title~content=t713926090

Influence of spacer length on the dielectric relaxation of a side chain liquid crystal polymer

Z. Z. Zhong[a]; D. E. Schuele[a]; W. L. Gordon[a]
[a] Department of Physics, Case Western Reserve University, Cleveland, Ohio, U.S.A.

To cite this Article Zhong, Z. Z. , Schuele, D. E. and Gordon, W. L.(1994) 'Influence of spacer length on the dielectric relaxation of a side chain liquid crystal polymer', Liquid Crystals, 17: 2, 199 — 209
To link to this Article: DOI: 10.1080/02678299408036560
URL: http://dx.doi.org/10.1080/02678299408036560

LIQUID CRYSTALS, 1994, VOL. 17, NO. 2, 199–209

Influence of spacer length on the dielectric relaxation of a side chain liquid crystal polymer

by Z. Z. ZHONG*, D. E. SCHUELE and W. L. GORDON
Department of Physics, Case Western Reserve University, Cleveland, Ohio 44106-7079, U.S.A.

(*Received 19 November 1992; accepted 27 October 1993*)

The dielectric relaxation study on a set of polyvinylether based cyanobiphenyl side chain liquid crystal polymers with three different alkyl spacer lengths of 7, 9, and 11 shows that the spacer decouples the motion of the mesogen from the polymer backbone so that both the low-frequency δ process and the high-frequency α process of the side group have been detected in smectic A phase. At a given temperature the relaxation frequency increases with spacer length for the α process. This trend is also observed for the δ process except for the longest spacer length.

1. Introduction

It is well known that a flexible spacer plays important roles in side-chain liquid crystal polymers (LCPs). Systematic investigations of the synthesis, characterization, and applications of side-chain liquid crystal polymers began only after Finkelman and co-workers proposed that a flexible spacer should be inserted between the polymer main chain and the mesogenic side groups to decouple the motions of the main-chain and side-groups in the liquid crystalline state [1, 2]. The numerous, previous investigations concerning the synthesis of polymers with low molar mass liquid crystals (LCs) attached to their backbones did not lead to a synthetic method which could systematically produce side-chain LCPs, since most involved polymers with mesogens attached directly to the polymer backbone [3].

The spacer, usually an alkyl chain $\text{-}(CH_2)_m\text{-}$, may function in a way that the main chain could do little to hinder the orientation of the mesogenic side group. In most cases, the glass transition temperature decreases with increasing spacer length in a similar manner to increasing the polymer backbone flexibility. Although a spacer helps to decouple the mesogenic groups from the main chain and that decoupling becomes more effective with increasing spacer length, this kind of decoupling is nevertheless incomplete.

The alkyl group does not carry a significant dipole [4] however, its flexibility allows internal reorientations between the backbone and the pendant liquid crystal mesogens, which often carry strong dipole moments and are dielectrically active. The spacer length influence on the molecular dynamics in a side-chain LCP system can therefore be detected by dielectric relaxation spectroscopy, measuring the relaxation processes of the liquid crystal side group attached to the backbone through different alkyl spacers. Spacer length influence on the dielectric relaxation has been compared before [5–9], however most of studies were conducted on the polyacrylate or polymethacrylate based side-chain LCP samples with an even number alkyl spacer. In this paper, dielectric measurements on three polyvinylether based cyanobiphenyl side-chain LCP samples, with the odd number spacer lengths of 7, 9, and 11, are reported.

* Author for correspondence.

0267–8292/94 $10·00

2. Experimental

The thermotropic side-chain LCP samples, Poly{ω-[(4-cyano-4'-biphenyl)oxy]alkyl vinyl ethers}s, were recently synthesized by V. Percec and co-workers using a cationic polymerization method in an attempt to elucidate the molecular engineering design mechanism in side-chain polymeric liquid crystals. The results demonstrate that the transformation of the nematic mesophase of the monomer into a smectic mesophase after polymerization occurs at the level of monomeric structural unit [10–13]. The molecular structure is shown in scheme 1, which contains a cyanobiphenyloxy mesogen attached via a flexible alkyl spacer to a polyvinylether backbone. Molecular weight was determined by gel permeation chromatography (GPC) [11], with degree of polymerization (*DP*) around 30. Three samples with three different spacer lengths *m* (7, 9 and 11) are denoted as C7DP30, C9DP30, and C11DP30, respectively. They all exhibit a smectic A (S_A) phase at room temperature, verified by a Nikon polarizing microscope with a custom built oven. Differential scanning calorimetric (DSC) measurements were taken with a DuPont 910 cell base incorporating a DuPont 990 thermal analyser at a $10\,K\,min^{-1}$ heating rate. The mesogenic phase transitions were recorded at the maximum of their endothermic peaks while glass transition temperatures (T_g) were recorded at the midpoint of the step change in the heat capacity. The DSC data was recorded with some digital equipment.

The dielectric sample cell was constructed of two parallel ITO (indium–tin–oxide, $20\,\Omega/\square$) glass plates, which allows for optical examination. The edge of the ITO plate was stripped using a mixture solution of hydrochloric and nitric acids. The two plates were glued together by a high temperature epoxy, separated by a 25 μm kapton spacer, to form a parallel-plate capacitor with the empty cell capacitance C_0 of 6–7 pF. The side-chain LCP sample was inserted on to the cell through capillary action, being placed on a hot stage in a vacuum chamber and heated above the isotropic temperature. The casting time for C7DP30 was about 3·5 h and slightly shorter for C9DP30 and C11DP30. The LC samples can be magnetically aligned since the mesogens in the side group have strong diamagnetic anisotropy. Both homeotropic (H-) and planar (P-, or homogeneous) alignments were achieved by slowly cooling the sample placed in a 7 Tesla superconducting magnet (Cryomagnetics, Inc.) from the isotropic (I) phase to S_A phase at room temperature. The cooling rate of $5\,K^{-1}$ was well controlled by a Lakeshore temperature controller together with a custom built ramp circuit. For the H-alignment, the cell was mounted with its layer normal parallel to the field; for P-alignment, perpendicular to the field [14].

The dielectric loss (G/ω) and capacitance (C) were measured at 17 frequencies (10 Hz–100 kHz, in a linear logarithm ratio) using an ultra-precision ratio-arm transformer bridge (CGA-83, C. Andeen and Assoc. [15]) at 5 K interval temperatures from 100 K to 400 K. For the aligned samples, the upper limit temperature was 370 K, well below the clearing points, to avoid destroying the alignments. The bridge's excitation voltage was chosen to be the least level ($\approx 0{\cdot}1$ V) to avoid disturbing the LCs macroscopic alignment and inducing additional dipole moments. The individual cell

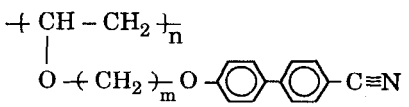

Scheme 1. Molecular structure of the polyvinyl-ether based cyanobiphenyl side-chain liquid crystal polymer (LCP) with the alkyl spacer length $m = 7$, 9, and 11.

was placed in a cryostat for data acquisition at low temperatures and a vacuum oven for data collection at elevated temperatures. The temperature was controlled by a Lakeshore DRC 82C controller with two platinum sensors, which can stabilize temperature at 10 mK to meet the isothermal conditions. The data acquisition steps were controlled by an HP-87 computer through an IEEE-488 bus interface [14].

3. Results and discussion

3.1. *DSC results*

The DSC measurement for each sample was repeated at least three times. Some transitions, such as molecular crystalline and semicrystalline, were absent from thermal scan following the initial scan. Figure 1 shows the second scan result for C7DP30, where the glass transition T_g is 290 K and the S_A–I transition is at 408 K. The phase transitions for the three studied samples are summarized in table 1.

As expected, the glass transition T_g decreases with increasing spacer length m, for example, T_g is 290 K for C7DP30 ($m=7$) and 282 K for C9DP30 ($m=9$). C11DP30 ($m=11$) has a T_g approximately the same as C9DP30. Each side-chain LCP sample establishes a smectic A mesophase, since these three samples have fairly long spacer lengths ($m=7$–11), which decouple the side-chain motion from the main chain polyvinyl ether. In contrast, the same cyanobiphenyl side-chain LCP samples with shorter spacer lengths ($m=2$, 3, and 4) hardly demonstrate an S_A phase [16]. The isotropic temperature T_I increases with increasing spacer length, i.e. $T_I \approx 408$, 422, and 435 K, respectively for $m=7$, 9, and 11. In short, given the approximately same *DP*, the

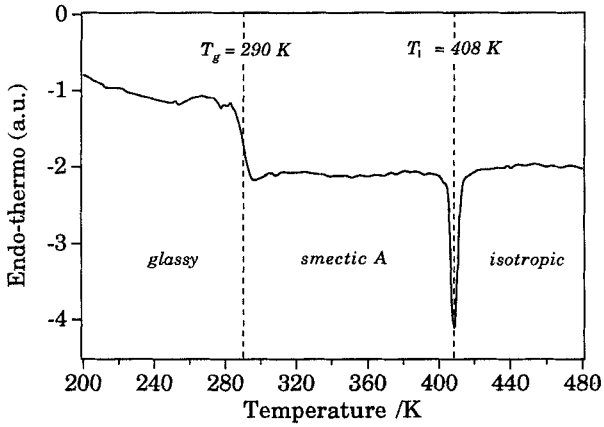

Figure 1. Differential scanning calorimetric (DSC) measurement for C7DP30 at a heating rate of about 10 K min^{-1}. This is a result of the second scan.

Table 1. Phase transitions in the studied side-chain LCP samples from DSC scan at 10 K min^{-1} heating rate.

Sample	$\bar{n}$ (*DP*)	*m*	Phase transitions/K†	$10^{-3} M_n$
C7DP30	30	7	g 290 S_A 408 I	10·3
C9DP30	32	9	g 282 S_A 422 I	11·6
C11DP30	30·6	11	g 282 C 295 S_A 435 I	11·97

† Glass; C, crystalline; S_A, smectic A; I, isotropic.

longer spacer length enlarges the temperature range of the mesophase. C11DP30, the longest spacer length sample, has a more complicated phase diagram, having a $T_C \approx 295$ K. The longest spacer length may sufficiently decouple the interaction between the backbone and LC side chain to possibly result in some microphase separation [3, 17–19].

3.2. *Dielectric constant and conductivity*

The dielectric constant $\varepsilon'(\omega) = C(\omega)/C_0$ and conductivity $\sigma(\omega) = \varepsilon_0 G(\omega)/C_0$ can be obtained from the dielectric measurement. Table 2 lists the dielectric constant ε' and conductivity σ for each sample at 1 kHz measuring frequency and at room temperature (≈ 295 K) as well as the corresponding empty cell capacitance C_0.

The dielectric constant increases with increasing spacer length, which can be attributed to the increase in the effective dipole moments. Here, the effective dipole moments mean those capable of being thermally activated to reorientate relatively freely. At a given temperature above T_g, the polymer chain together with the LC side group containing permanent dipoles tends to be thermally activated more easily for the lower T_g material, which has a longer spacer length in this case. The conductivity (d.c. + a.c.) for each sample is of the order of 10^{-9} S m^{-1} at 1 kHz and room temperature. There seems no obvious correlation in the conductivities among the three samples. C7DP30 has a conductivity of $1{\cdot}7 \times 10^{-9}$ S m^{-1}, smaller than that of C9DP30 with $5{\cdot}4 \times 10^{-9}$ S m^{-1}. However, C11DP30 with the longest spacer length has the least conductivity of $1{\cdot}1 \times 10^{-9}$ S m^{-1}.

3.3. *Dielectric relaxation spectrum overview*

Dielectric relaxation studies on cyanobiphenyl side-chain LCP were first investigated by Kresse and co-workers based on polyacrylate [5, 20, 21], polymethacrylate [22], and polysiloxane [23]. Figure 2 gives the dielectric loss spectra of the H-aligned C7DP30 at 10 Hz, 1 kHz, and 100 kHz, and the error bar is within the graphic line size due to the special ultra-precision ratio-arm capacitance bridge. The dielectric spectrum of the side-chain LCP system in the whole measured temperature range ($T < T_I$) shows four relaxation processes. There are two relaxations below the calorimetric T_g, labelled by β and γ with decreasing temperature. The S_A region ($T_g < T < T_I$) contains two typical processes in the side-chain LCP mesophase, labelled by δ and α in decreasing temperature. This kind of loss peak labelling (δ, α with decreasing temperature) is contrary to the traditional nomenclature for polymeric materials ($\alpha, \beta, \gamma, \ldots$, with decreasing temperature), but has been widely accepted by authors in the LCP field. [4, 24–26]

Both β and γ relaxations occur below the glass transition of the side-chain LCP sample, where the polymer backbone chain is essentially frozen. These two low-

Table 2. Dielectric constants and conductivities for the unaligned samples at room temperature (≈ 295 K) and 1 kHz measuring frequency.

Unaligned sample	C_0/pF	ε'	$\sigma \times 10^9$/S m^{-1}
C7DP30	7·0	2·8	1·7
C9DP30	7·0	3·1	5·4
C11DP30	6·0	3·3	1·1

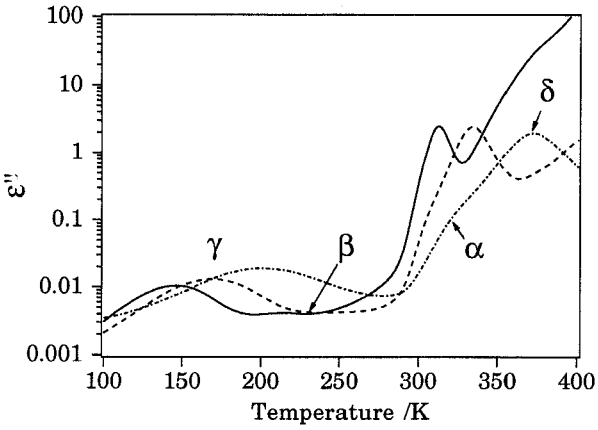

Figure 2. Dielectric loss spectra for the homeotropically (H-) aligned C7DP30 at 10 Hz (——), 1 kHz (- - - - -), and 100 kHz (– · – · – · –). The four processes are labelled as δ, α, β, and γ in decreasing temperature. The error bar is within the graphic line size due to the special ratio-arm capacitance bridge.

temperature relaxations are very similar to those in poly{vinyl methyl ether} [27] and usually involve only local motions of some segments either in the main chain or in the side chain [28]. Although they are almost independent of the alignment and the spacer length, there are slight deviations in the loss amplitude for different alignment configurations. The loss amplitude in the γ relaxation increases with increasing temperature and the relaxation frequency at a given temperature is much higher than that in the β relaxation. The broad γ process may combine a few different local motions, including some in the cyanobiphenyl group [29] in the side chain, and has an activation energy of about 40 kJ mol^{-1}. The β peaks are merged with the α process at higher frequencies (> 1 kHz), where the glass transition of the polymer appears. As follows in this paper, the discussion will be focused on the two major relaxation processes α and δ.

3.4. α *and* δ *relaxations*

In the S_A region, there are two major dielectric relaxation processes, a broad high-frequency α peak and a narrow low-frequency δ peak. Figure 3 shows the dielectric loss factor ε'' for the unaligned (U-) and H-aligned C7DP30 from 305–325 K. The δ peaks in the H-alignment are dramatically enhanced compared with the unaligned and the α peaks are almost absent. In contrast, in figure 4 for C9DP30, the δ peaks are suppressed in the P-alignment while the α peaks are increased. These are typical dielectric loss behaviours in a side-chain LCP system [30–36].

The Fuoss–Kirkwood function [37], a symmetric empirical lineshape, has been used to fit the dielectric relaxation spectrum in the side-chain LCP [4, 26, 34, 38]. In the temperature range from 295–330 K where the samples are in the S_A phase, the dielectric loss spectrum $\varepsilon''(\omega) = G(\omega)/\omega C_0$, is thought to consist of a low frequency δ peak, a high frequency α peak, and a DC conductance,

$$\varepsilon''(\omega) = G(\omega)/\omega C_0 = (\sigma_{DC}/\omega\varepsilon_0) + \sum_{\delta,\alpha} \varepsilon''_{mi}\,\mathrm{Sech}\,[\beta_i \ln(\omega/\omega_{Ri})], \tag{1}$$

where angular frequency $\omega = 2\pi f$ and relaxation frequency $\omega_R = 2\pi f_R$; σ_{DC} is a DC conductivity; ε''_{mi} is the amplitude of the imaginary part of the complex dielectric constant $\varepsilon^* = \varepsilon' - i\varepsilon''$; β lies between 0 and 1 and is a width distribution parameter and is

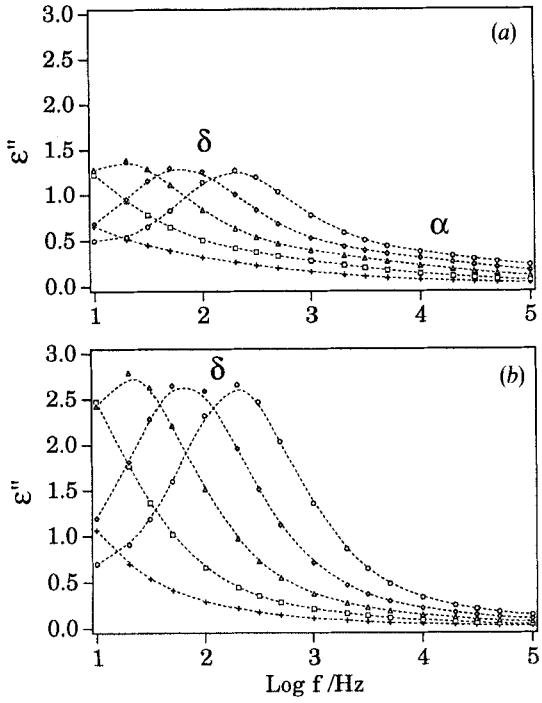

Figure 3. The δ and α processes in C7DP30 from 305–325 K (+, 305 K; □, 310 K; △, 315 K; ◇, 320 K; ○, 325 K): (*a*) unaligned (U-); (*b*) homeotropically aligned (H-). The dash lines represent the Fuoss–Kirkwood fitting results using equation (1), and the parameter variances are listed in table 3.

equal to 1·14/(width of loss peak at half-height). The Fuoss–Kirkwood function reduces to a Debye-type relaxation when $\beta = 1$. The dielectric relaxation strength for each process, $\Delta\varepsilon'$, the difference in the dielectric constants at low-end and high-end frequencies and proportional to the amount of dipole moments involved in the relaxation, can be expressed in terms of two fitting parameters [4],

$$\Delta\varepsilon' \equiv \varepsilon'_0 - \varepsilon'_\infty = 2\varepsilon''_m/\beta. \tag{2}$$

The results from Fuoss–Kirkwood data fitting (equation (1)), including the parameter variances, for all three samples at 315 K are listed in table 3. The DC conductivity σ_{DC} of the aligned sample seems larger than that of the unaligned, for instance, σ_{DC} is $10{\cdot}1 \times 10^{-12}\,\mathrm{S\,m^{-1}}$ for the unaligned C9DP30 while $18{\cdot}3 \times 10^{-12}\,\mathrm{S\,m^{-1}}$ for the P-aligned. Overall, the DC conductivity increases with increasing the spacer length, however, this is very dependent on the impurities in a particular sample. The relaxation frequency f_R for both α and δ process is basically independent of the specific alignment configuration except the δ peak shifts slightly towards a higher frequency position in P-aligned samples (see figure 4 and table 3), which is predicted by the four-mode theory described by Williams and co-workers [35, 38].

The two major relaxation processes are usually interpreted in terms of rotational dynamic theory [4, 35, 39–41]. The theory only requires that the conditional probability distribution function be expanded in terms of correlation functions of the motion, which are not specific to any rotational (diffusion) model [42, 43]. In side-chain polymeric liquid crystal materials, steric hindrance prevents a simple reorientation of

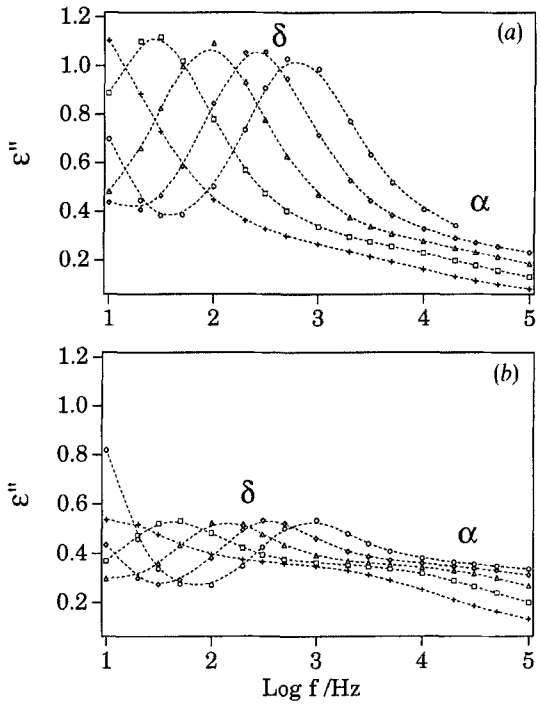

Figure 4. The δ and α processes in C9DP30 from 305–325 K (+, 305 K; □, 310 K; △, 315 K; ◇, 320 K; ○, 325 K): (*a*) unaligned (U-); (*b*) planarly or homogeneously aligned (P-). The dash lines represent the Fuoss–Kirkwood fitting results using equation (1), and the parameter variances are listed in table 3.

the side-chain mesogenic unit about its long or short axes. Reorientations of the unit, if any, are possible only as a result of highly cooperative motions involving both rotation and translation of the unit and of the neighbouring environment.

The longitudinal component of the dipole moment in the uniaxial side chain mesogen μ_l is approximately 4·2 Debye [44], which comes from its cyanobiphenyl end group (–C≡N), and is much larger than the transverse component μ_t, approximately 2 Debye from the oxy-group (–O–). The low frequency δ peak can be assigned to the 180° rotation of the longitudinal dipole moment in the mesogenic group about its short axis. In the smectic A phase, it is possible for the side group to flip around the polymer backbone, hopping from one smectic layer to another. The high frequency and broad α process can be thought to involve both longitudinal and transverse dipole moments in the mesogenic group, combined into a few different rotational modes. Since the amplitude of the α peak is much smaller than that of the δ peak and is almost uncoupled from the driving electric field in the H-aligned samples, the major contribution to the α process comes from the transverse dipole moments ($\mu_t < \mu_l$) rotating about the mesogens' long axis.

3.5. *Spacer length effects*

In their dielectric investigations on two polyacrylate-based cyanophenyl benzoate samples with spacer lengths of 2 and 6, Kresse and co-workers have concluded that an increase of the spacer length ensures a strong increase of the relaxation frequency, i.e. with increasing spacer length we have stronger decoupling of the main chain from the

Table 3. Results from Fuoss–Kirkwood data fitting for all the studied samples at 315 K by using equation (1).

Sample	Align	$\sigma_{DC}/10^{-12}$ S m^{-1}	δ peak				α peak				Parameter variances/per cent
			log f_R	ε''_m	β	$\Delta\varepsilon'$	log f_R	ε''_m	β	$\Delta\varepsilon'$	
C7DP30	U-	2·5	1·24	1·25	0·73	3·40	3·07	0·26	0·32	1·66	±6
	H-	6·0	1·31	2·67	0·80	6·72	3·02	0·13	0·31	0·87	±4
C9DP30	U-	10·1	1·95	0·97	0·83	2·34	3·81	0·24	0·31	1·58	±8
	P-	18·3	2·11	0·34	0·92	0·75	3·92	0·34	0·30	2·22	±2
C11DP30	U-	3·4	1·35	0·22	0·54	0·82	4·08	0·04	0·26	0·29	±4
	H-	10·0	1·39	0·20	0·51	0·80	—	—	—	—	±10
	P-	33·9	2·39	0·03	0·54	0·12	3·59	0·09	0·20	0·88	±6

side group [5]. The further study on the δ process of the same samples under high hydrostatic pressure indicates that the δ process is closely correlated with the glass relaxation [6].

Generally speaking, at a given temperature the longer spacer length can decouple the LC side group from the motion of the polymer backbone more efficiently so that the side group would reorient faster and the relaxation rate f_R would be higher. This holds true for the α process for the three samples with different alkyl spacer lengths from 7 to 11, for instance, in table 3 for the temperature at 315 K, the f_R increases from $10^{3\cdot07}$ to $10^{4\cdot08}$ Hz.

This kind of trend is also observed for the δ process in C7DP30 and C9DP30, for example the f_R for the unaligned C7DP30 is $10^{1\cdot24}$ Hz at 315 K while the unaligned C9DP30 is $10^{1\cdot95}$ Hz—a 0·71 decade difference in relaxation frequency (see table 3 and figure 5). Unfortunately, it does not hold for C11DP30, the longest spacer length sample among those studied. The f_R of the δ process in the unaligned C11DP30 is $10^{1\cdot35}$ Hz, smaller than that $10^{1\cdot95}$ Hz in the unaligned C9DP30, even though C11DP30 has the higher f_R in the α process. This 'abnormal' phenomenon cannot be simply attributed to the difference in *DP* (see table 1, *DP* for C9DP30 is on average 32 and C11DP30 is 30·6), since such a small difference in molecular weight would not be expected to effect the corresponding relaxation this much. The width parameter β in the δ peak of C11DP30 is around 0·54, much smaller than that of C7DP30 or C9DP30, in other words, the δ process of C11DP30 is no longer Debye-like and must be combined with some other processes. As mentioned before, there might be an intramolecular microphase separation of the side group from the polymer backbone [3, 17, 45] in the longest spacer C11DP30. So, the microscopic structure in C11DP30 may include not only the conventional side-chain liquid crystal polymer system but also a phase separated sub-system. As a result, the δ reorientation relaxation in such a nonhomogeneous structure could be slowed down in a complicated way compared with the pure

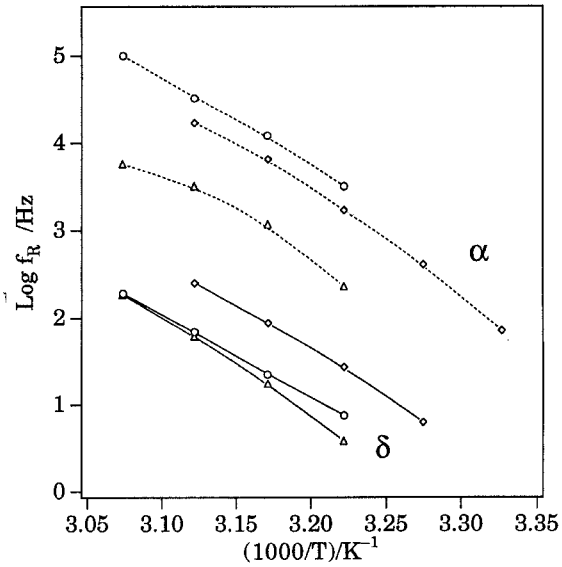

Figure 5. Arrhenius plot for all the unaligned samples. △, C7DP30; ◇, C9DP30; ○, C11DP30. Solid line is for the δ relaxation and dash line is for the α relaxation.

side-chain LCP structure. On the other hand, the longest spacer sample has less topological restriction compared with other two shorter spacer samples, and the reorientation of the longitudinal dipole moment about the short axis does not necessarily require for whole side group to rotate around the polymer main chain. This 'localized' rotational motion can sometimes be slowed down.

The dielectric strength $\Delta\varepsilon'$, calculated according to equation (2), decreases reasonably with increasing spacer length since $\Delta\varepsilon'$ is proportional to the density of dipole moments within the sample and therefore the longer spacer sample has a lower dipole density. Figure 5 is the Arrhenius plot for the three unaligned samples, which clearly shows that in the α process the longer spacer length has the higher relaxation frequency at fixed temperature; however in the δ process the curve of the longest spacer C11DP30 lies between the curves of C7DP30 and C9DP30. On the average in the plotted temperature region, the activation energy of the δ process is approximately 217, 200, and 182 kJ mol^{-1} respectively for C7DP30, C9DP30, and C11DP30; the activation energy of the α process is estimated to be 179, 221, and 199 kJ mol^{-1}.

4. Conclusions

Dielectric relaxation study has been conducted on three smectic polyvinylethers containing cyanobiphenyl side group via alkyl spacer lengths of 7, 9, and 11. The two major relaxation processes (α and δ) have been confirmed in different alignment states. At a given temperature the relaxation frequency increases with increasing the spacer length for the α process, which is consistent with previous work by Kresse *et al.* This trend is also observed for the δ process except for the longest spacer length, on which further investigation is needed to verify the hypothesis of the microphase separation in such a smectic A side-chain liquid crystal polymer.

The authors are indebted to Professor V. Percec for providing the side-chain liquid crystal polymer samples and Professor C. Rosenblatt for the use of the superconducting magnet. The authors also benefited from many helpful dicussions with Dr R. B. Akins and Mr D. Gu. This work was supported by NSF Materials Research Group at CWRU under Grant DMR 89-01845. Partial support for Z.Z.Z. by NSF/S&TC Advanced Liquid Crystalline Optical Materials (ALCOM) under Grant DMR 89-20147 is also acknowleged.

References

[1] FINKELMAN, H., HAPP, M., PORTUGALL, M., and RINGSDORF, H., H., 1978, *Makromolek. Chem.*, **179**, 254.

[2] FINKELMAN, H., RINGSDORF, H., SIOL, W., and WENDORFF, J. H., 1978, *Mesomorphic Order in Polymers and Polymerization in Liquid Crystalline Media ACS Symp. Ser.*, Vol. 74, edited by A. Blumstein (American Chemical Society, Washington, D.C.), p. 22.

[3] PERCEC, V., and PUGH, C., 1989, *Side-Chain Liquid Crystal Polymers*, edited by C. B. McArdle (Chapman & Hall), Chap. 3, pp. 30–105 and references cited therein.

[4] HAWS, C. M., CLARK, M. G., and ATTARD, G. S., 1989, *Side-Chain Liquid Crystal Polymers*, edited by C. B. McArdle (Chapman & Hall), Chap. 7, pp. 196–227 and references cited therein.

[5] KRESSE, H., TENNSTEDE, E., and ZENTEL, R., 1985, *Makromolek. Chem. rap. Commun.*, **6**, 261.

[6] HEINRICH, W., and STOLL, B., 1985, *Coll. Polym. Sci.*, **263**, 895.

[7] ZENTEL, R., STROBL, G. R., and RINGSDORF, H., 1985, *Macromolecules*, **18**, 960.

[8] PARNEIX, J. P., NIEUMO, R., LEGRAND, C., LE BARNY, P., and DUBOIS, J. C., 1987, *Liq. Crystals*, **2**, 167.

[9] VALLERIEN, S. U., KREMER, F., and BOEFEL, C., 1989, *Liq. Crystals*, **4**, 79.

[10] PERCEC, V., and LEE, M., 1991, *Macromolecules*, **24**, 1017.

[11] PERCEC, V., and LEE, M., 1991, *Macromolecules*, **24,** 2780.
[12] PERCEC, V., LEE, M., and JONSSON, H., 1991, *J. polym. Sci.* A, **29,** 327.
[13] LEE, M., 1992, Ph.D. Thesis, Case Western Reserve University, Cleveland, Ohio.
[14] ZHONG, Z. Z., 1993, Ph.D. Thesis, Case Western Reserve University, Cleveland, Ohio.
[15] ANDEEN, C. G., 1971, Ph.D. Thesis, Case Western Reserve University, Cleveland, Ohio.
[16] PERCEC, V., and LEE, M., 1991, *J. macromolek. Sci. Chem.*, **28,** 651.
[17] LIPATOV, YU. S., TSUKRUK, V. V., and SHILOVE, V. V., 1983, *Polymer Commun.*, **24,** 75.
[18] DOANE, J. W., 1990, *Liquid Crystals: Applications and Uses*, edited by B. Badhadur (World Scientific), Chap. 14, pp. 361–395.
[19] ZHONG, Z. Z., SCHUELE, D. E., GORDON, W. L., ADAMIC, K. J., and AKINS, R. B., 1992, *J. polym. Sci.* B, **30,** 1443.
[20] KRESSE, H., and TALROSE, R. V., 1981, *Makromolek. Chem. rap. Commun.*, **2,** 369.
[21] KRESSE, H., and SHIBAEV, V. P., 1984, *Makromolek. Chem. rap. Commun.*, **5,** 63.
[22] KRESSE, H., KOSTROMIN, S., and SHIBAEV, V. P., 1982, *Makromolek. Chem. rap. Commun.*, **3,** 509.
[23] KRESSE, H., WIEGELEBEN, A., and KRÜCKE, B., 1988, *Acta pol.*, **39,** 583.
[24] ATTARD, G. S., MOURA-RAMOS, J. J., and WILLIAMS, G., 1987, *J. polym. Sci. polym. Phys. Ed.*, **25,** 1099.
[25] WILLIAMS, G., NAZEMI, A., KARASZ, F. E., HILL, J. S., LACEY, D., and GRAY, G. W., 1991, *Macromolecules*, **24,** 5134.
[26] BORMUTH, F. J., and HAASE, W., 1988, *Liq. Crystals*, **3,** 881.
[27] PATHMANATHAN, K., and JOHARI, G. P., 1987, *J. polym. Sci.* B, **25,** 379.
[28] SMITH, G. D., LIU, F., DEVEREAUX, R. W., and BOYD, R. H., 1992, *Macromolecules*, **25,** 703.
[29] ZELLER, H. R., 1981, *Phys. Rev.* A, **23,** 1434; 1982, *Phys. Rev. Lett.*, **48,** 334.
[30] BORMUTH, F. J., and HAASE, W., 1983, *Polymeric Liquid Crystals*, edited by A. Blumstein (Plenum Press), p. 313.
[31] PRANOTO, H., BORMUTH. F. J., HAASE, W., KIECHLE, U., and FINKELMANN, H., 1986, *Makromolek Chem.*, **187,** 2453.
[32] BORMUTH, F. J., and HAASE, W., 1987, *Molec. Crystals liq. Crystals*, **148,** 1.
[33] BORMUTH, F. J., MÜHLBERGER, B., and HAASE, W., 1989, *Makromolek. Chem. rap. Commun.*, **10,** 231.
[34] ATTARD, G. S., and WILLIAMS, G., 1986, *Liq. Crystals*, **1,** 253.
[35] ARAKI, K., ATTARD, G. S., KOZAK, A., WILLIAMS, G., GRAY, G. W., LACEY, D. and NESTOR, G., 1988, *J. chem. Soc. Faraday Trans. II*, **84,** 1067.
[36] MOURA-RAMOS, J. J., and WILLIAMS, G., 1991, *Polymer*, **32,** 909.
[37] FUOSS, R. M., and KIRKWOOD, J. G., 1941, *J. Am. chem. Soc.*, **63,** 385.
[38] ATTARD, G. S., 1986, *Molec. Phys.*, **58,** 1087.
[39] MAIER, V. W., and SAUPE, A., 1959, *Z. Naturf.* (*a*), **14,** 882.
[40] NORDIO, P. L., RIGATTI, G., and SEGRE, U., 1973, *Molec. Phys.*, **25,** 129.
[41] FERRARINI, A., POLIMENO, and NORDIO, P. L., 1993, *Liq. Crystals*, **14,** 169.
[42] KOZAK, A., MOSCICKI, J. K., and WILLIAMS, G., 1991, *Molec. Crystals liq. Crystals*, **201,** 1.
[43] KOZAK, A., and MOSCICKI, J. K., 1992, *Liq. Crystals*, **12,** 377.
[44] KLINBIEL, R. T., GENOVA, D. J., CRISWELL, T. R., and VAN METER, J. P., 1974, *J. Am. chem. Soc.*, **96,** 7651.
[45] PERCEC, V., and TOMAZOS, D., 1989, *J. polym. Sci.* A, **27,** 999.